

<https://doi.org/10.1038/s41526-025-00548-y>

# Staphylococcal enterotoxin C2 rescued simulated microgravity-induced bone loss and the trans-differentiation of BMSCs into adipocytes

Check for updates

Nan Hou<sup>1,2,3,5</sup>, Zhengmeng Yang<sup>3,5</sup>, Haixing Wang<sup>4</sup>, Xuan Lu<sup>3</sup>, Shanshan Bai<sup>3</sup>, Yaofeng Wang<sup>3</sup>, Sien Lin<sup>1,2</sup>, Micky D. Tortorella<sup>1,3</sup>✉, Lu Feng<sup>1,3</sup>✉ & Gang Li<sup>1,4</sup>✉

Exposure to microgravity decreases bone volume and increases marrow fat, partly due to impaired BMSC osteogenesis and enhanced adipogenesis. Staphylococcal enterotoxin C2 (SEC2) can influence BMSC differentiation, potentially promoting osteogenesis. This study investigated SEC2's effects on bone loss and marrow fat in hindlimb suspension (HLS) mice and BMSC differentiation under simulated microgravity. Results showed SEC2 alleviated bone deterioration and reduced marrow adiposity, promoting osteogenic over adipogenic differentiation by activating ERK/β-catenin signaling pathways. SEC2 increased ERK phosphorylation and β-catenin nuclear translocation, with effects diminished upon β-catenin knockdown. These findings reveal a novel mechanism by which SEC2 modulates BMSC fate under microgravity, highlighting its potential as a therapeutic agent for preventing bone loss and marrow adiposity in microgravity conditions.

The human body has evolved under the constant influence of Earth's gravity. Numerous studies have demonstrated that exposure to microgravity in space has a significant impact on various physiological systems. The microgravity environment in space leads to bone and muscle loss and atrophy, which may have negative effects on the health and performance of astronauts. Extensive research has been conducted to understand the underlying mechanisms through which microgravity or simulated microgravity (SMG) affects human tissue and cells. In terms of the musculoskeletal system, changes in gravity result in a decrease in trabecular bone volume and formation rate, as well as an increase in fat content in the bone marrow<sup>1</sup>. Additionally, muscle mass, including the soleus-gastrocnemius, anterior calf, hamstrings, quadriceps, and intrinsic back muscles, is also reduced under microgravity conditions<sup>2</sup>. Furthermore, microgravity affects the expression levels of numerous mRNAs and microRNAs involved in mechanotransduction, cell migration, angiogenesis, and osteogenic differentiation within the musculoskeletal system<sup>3</sup>.

Bone loss observed during long-term spaceflight is partially attributed to the detrimental effect of microgravity on osteogenic cells, such as osteoblasts and mesenchymal stem cells (MSCs). MSCs are multipotent and can differentiate into various cell types, including osteoblasts, chondrocytes, myocytes, and adipocytes, in response to environmental changes or tissue regeneration needs. Microgravity induces the commitment of MSCs towards adipocytes instead of osteoblasts, resulting in decreased bone formation and increased adipose regeneration. Microgravity inhibits the expression of osteogenic genes, such as collagen family members, alkaline phosphatase (ALP), and runt-related transcription factor 2 (RUNX2), ultimately affecting bone microarchitectures by altering mineral deposition and collagen synthesis<sup>4</sup>. On the other hand, microgravity activates adipose tissue synthesis and upregulates the expression of key adipogenic genes, including adiponectin (CFD), leptin (LEP), CCAAT/enhancer binding protein (CEBP), and peroxisome proliferator-activated receptor gamma (PPAR $\gamma$ ). As a result, the route through which bone marrow mesenchymal stem cells

<sup>1</sup>Stem Cells and Regenerative Medicine Laboratory, Li Ka Shing Institute of Health Sciences, Prince of Wales Hospital, The Chinese University of Hong Kong, Shatin, Hong Kong SAR, PR China. <sup>2</sup>Musculoskeletal Research Laboratory, Department of Orthopaedics & Traumatology, Faculty of Medicine, Prince of Wales Hospital, The Chinese University of Hong Kong, Shatin, Hong Kong SAR, PR China. <sup>3</sup>Centre for Regenerative Medicine and Health, Hong Kong Institute of Science & Innovation, Chinese Academy of Sciences, Hong Kong SAR, PR China. <sup>4</sup>Institute of Biomedicine and Biotechnology, Shenzhen Institute of Advanced Technology, Chinese Academy of Sciences, Shenzhen, Guangdong, PR China. <sup>5</sup>These authors contributed equally: Nan Hou, Zhengmeng Yang.

✉ e-mail: [m.tortorella@crmh-cas.org.hk](mailto:m.tortorella@crmh-cas.org.hk); [lufeng@link.cuhk.edu.hk](mailto:lufeng@link.cuhk.edu.hk); [gangli@cuhk.edu.hk](mailto:gangli@cuhk.edu.hk)

(BMSCs) differentiate into osteoblasts is disrupted, potentially impairing bone homeostasis.

Staphylococcal enterotoxins C2 (SEC2) belongs to a group of heat-resistant toxins known as Staphylococcal enterotoxins (SEs), which have diverse biological effects. SEC2 has the ability to stimulate T-cell growth and trigger the production of various cytokines, such as interferon-gamma (IFN $\gamma$ ), interleukin-I (IL-1), and interleukin-II (IL-2). These cytokines can significantly impact the osteogenic differentiation of MSCs. In our previous study, we found that administration of SEC2 effectively activates T cells, increases nitric oxide production, activates the p38/MAPK pathway, and enhances Runx2 expression, ultimately leading to an increased trabecular bone mass in ovariectomized (OVX) mice. Additionally, IFN $\gamma$ , secreted by T cells, also plays a crucial role in the regulatory process of SEC2 on bone homeostasis<sup>5</sup>. However, the specific mechanism by which SEC2 regulates bone homeostasis under SMG conditions remains unclear. Therefore, the objective of this study was to investigate the role of SEC2 in maintaining the homeostasis of weight-bearing bones in a microgravity environment. The model of mice in hindlimb suspension (HLS), along with the tissue culture system on a random position machine (RPM), were both employed to mimic the SMG conditions both in vivo and in vitro, respectively. Consecutively, we explored the underlying regulation mechanism of SMG on bone deterioration and MSCs cell fate determination.

## Results

### SEC2 rescued mice femoral bone loss induced by microgravity simulated by hind limb suspension

In order to simulate the effects of microgravity on weight-bearing bones, we utilized the HLS mouse model. To assess the microarchitectures and characteristics of the trabecular bones in the distal femurs of mice, we employed micro-computer tomography (micro-CT) analysis, comparing control mice to those subjected to HLS with or without SEC2 treatment. The findings revealed that microgravity resulted in a reduction of trabecular bone mass in the distal femurs of mice. However, this effect was significantly mitigated when SEC2 was administered, as evidenced by the restoration of both microstructure and bone mass (Fig. 1A). The HLS group exhibited decreased bone structural parameters, including bone volume/total volume (BV/TV), bone mineral density (BMD), and trabecular thickness (Tb.Th), in comparison to the control group. Notably, the application of SEC2 elevated these parameters (Fig. 1B–D). Notably, SEC2 administration in control mice without HLS intervention did not significantly affect bone mass or microstructural parameters. This indicates that the restorative effect of SEC2 on bone mass is highly dependent on the microgravity environment (Supplementary Fig. 1). Immunohistochemistry (IHC) staining further demonstrated that the expression levels of osteogenic markers including osteocalcin (OCN) and osteopontin (OPN) were downregulated in the femoral trabecular bone following HLS treatment. Nevertheless, these markers were restored to normal levels after SEC2 administration (Fig. 1E, F).

### Bone marrow adiposity increase was reversed by SEC2 treatment in hind limb suspension mice

The impact of microgravity on the adipose content in the bone marrow of weight-bearing femurs was assessed using immunofluorescence staining. Femur bone marrow samples from different groups were stained with goat anti-perilipin antibody, which helps to reveal the content and structure of lipid droplets in adipocytes. The staining results showed a significant increase in adipose tissue in the bone marrow following HLS treatment, in comparison to the control group. However, the administration of SEC2 effectively reduced the adipose accumulation in bone marrow (Fig. 2A). Additionally, representative images of femur sections stained with hematoxylin & eosin supported these findings, demonstrating an increase in adipocytes under HLS conditions, which was suppressed in the HLS+SEC2 group (Fig. 2B). Moreover, the semi-quantitative analysis revealed a significant increase in the number of adipocytes as well as the adipose volume/total volume (AV/TV) ratio in the bone marrow of the HLS group,

compared to the control group. However, both of these parameters were significantly reduced after SEC2 treatment (Fig. 2C, D).

### SEC2 ameliorated the fate shift of BMSCs into adipocytes under simulated microgravity conditions

In our in vivo study, we observed a deterioration in the bone formation in the femoral bone and bone marrow adiposity upon stimulation with SMG. However, these changes were abolished with the treatment of SEC2. Based on these findings, we hypothesized that SEC2 may regulate the shift in cell fate of BMSCs from osteoblasts to adipocytes under microgravity conditions. To investigate this, we utilized a RPM to randomly alter the orientation of BMSCs relative to the gravity vector (Fig. 3A). The BMSCs were grown in an osteoblast/adipocyte (OB/AD) induction medium at a 1:1 ratio and were then stained with Oil red O (ORO) and Alizarin Red S (ARS) to assess adipogenic and osteogenic differentiation, respectively. The results showed that SMG suppressed BMSCs' ability to differentiate into osteoblasts while enhancing their adipogenesis. Notably, the administration of SEC2 effectively reversed this cell fate shift under SMG conditions (Fig. 3B). The quantification of lipid accumulation indicated a 67% increase in the adipogenic activity of BMSCs under SMG. However, administration of SEC2 resulted in a 30% reduction of this effect (Fig. 3C). In parallel, quantification of Alizarin Red S staining showed a 30% decrease in the osteogenic activity of BMSCs under SMG, while SEC2 recovered it by 20% (Fig. 3D). Additionally, the mRNA levels of adipogenesis markers including Ppary, Cebpa and Leptin were elevated under SMG, while the osteogenesis markers including Alp, Col1a1 and Runx2 were suppressed. However, the addition of SEC2 significantly reversed the trend in protein expression, respectively (Fig. 3E, F).

### SEC2 reactivated Erk/β-catenin signaling pathway under microgravity

Previous research has demonstrated that the Erk/β-catenin signaling pathway becomes deactivated in the presence of microgravity<sup>6</sup>. Our study also found that when exposed to SMG, there was a decrease in the relative ratio of phosphorylated-Erk1/Erk1 (p-Erk1/Erk1) and phosphorylated-Erk2/Erk2 (p-Erk2/Erk2). Furthermore, the reduced levels of cytosolic β-catenin and the lowered nucleus/cytosolic ratio indicated suppressed β-catenin signaling following SMG treatment. Interestingly, SEC2 was observed to partially counteract the reduction in Erk and β-catenin signaling (Fig. 4A–E, and Supplementary Fig. 2). Immunofluorescence staining images further supported the role of SEC2 in restoring the impaired nucleus translocation of Erk and β-catenin in the presence of SMG (Fig. 4F).

### Knockdown of β-catenin diminished the promoting effect of SEC2 on the fate specification of BMSCs

To further confirm the role of Erk/β-catenin signaling in the cell fate determination of BMSCs under SMG conditions with SEC2 treatment, we performed experiments using BMSCs with β-catenin siRNA knockdown. These cells were then subjected to OB/AD induction medium to assess their trans-differentiation ability. The results of Oil Red O and Alizarin Red S staining demonstrated that in the siNC group, SEC2 counteracted the increased adipogenesis and decreased osteogenesis activity induced by SMG in BMSCs. However, when siβ-catenin was applied, the inhibitory effect on adipogenesis and the promoting effect on osteogenesis of SEC2 were significantly ameliorated (Fig. 5A). The semi-quantitative analysis of the ORO and ARS staining further supported our conclusions (Fig. 5B, C). Additionally, the results of quantitative real-time PCR analysis indicated that siβ-catenin knockdown could attenuate the inhibitory effect of SEC2 on the mRNA expression levels of adipogenesis markers induced by SMG (Fig. 5D), as well as the promoting effect of SEC2 on SMG-inhibited expression of osteogenesis markers (Fig. 5E).

## Discussion

Our study revealed the deteriorating impact of a SMG environment on the microstructure of weight-bearing femoral trabecular bone in HLS mice.

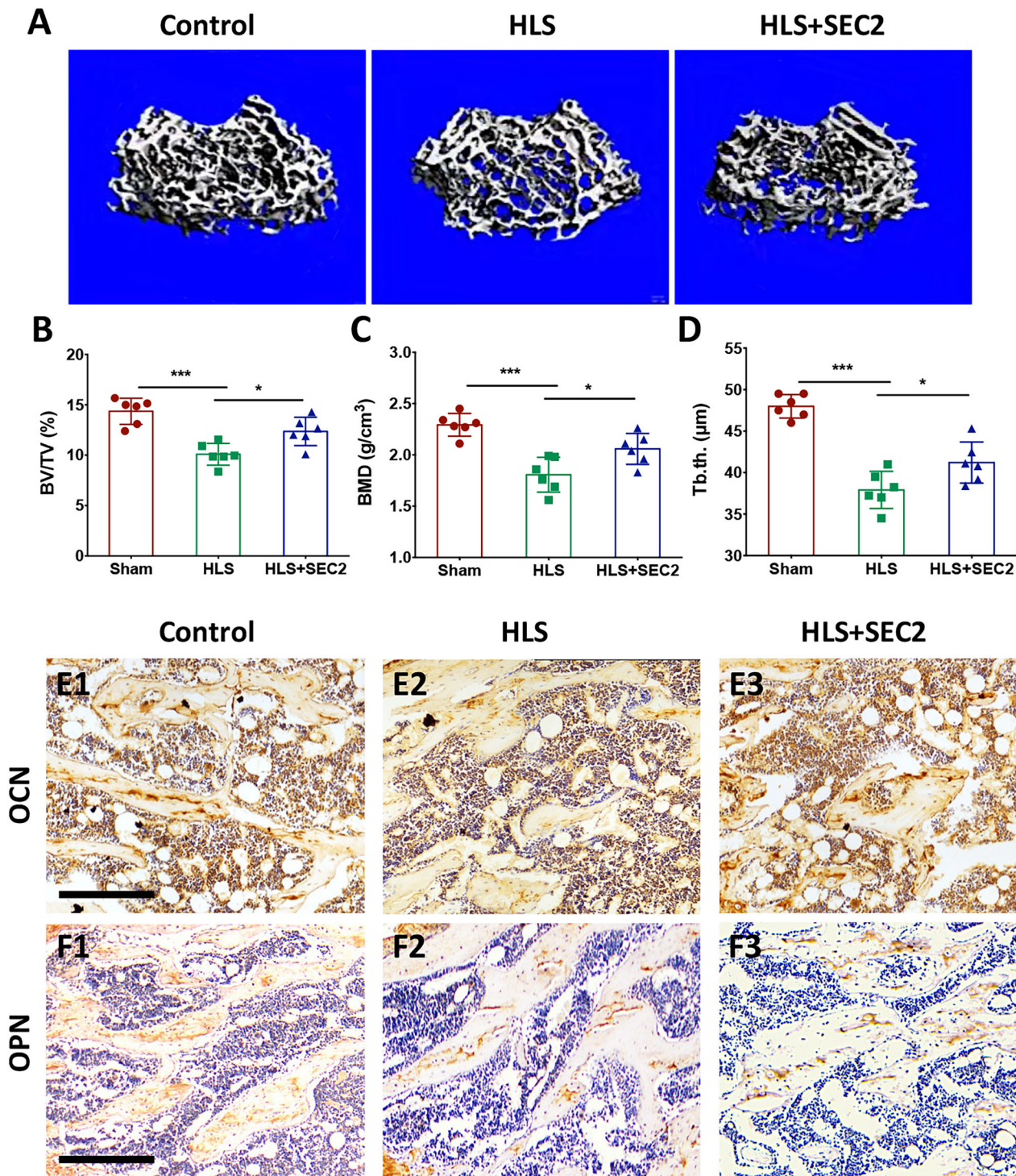


**Fig. 1 | Microstructure properties of the trabecular bone of hindlimb suspension (HLS) mice after SEC2 treatment.** A Three-dimensional reconstruction of trabecular bone in the distal metaphysis of HLS mice after SEC2 treatment. Microstructure parameters including bone volume/tissue volume (BV/TV) (B), bone

mineral density (BMD) (C) and trabecular thickness (Tb.Th) (D). Data were shown as mean  $\pm$  SD ( $n = 6$ ;  $^*p < 0.05$ ,  $^{**}p < 0.01$ ,  $^{***}p < 0.001$ ). Representative images of femoral metaphysis with IHC staining using osteocalcin (OCN) (E) and osteopontin (OPN) (F) antibodies. Scale bar: 50  $\mu$ m.

However, the administration of SEC2 treatment effectively reversed this deterioration. Additionally, SEC2 was found to be successful in mitigating the accumulation of bone marrow adipose tissue observed in HLS mice. Furthermore, we discovered that SMG altered the fate of BMSCs, causing them to differentiate into adipocytes instead of osteoblasts. Under SMG conditions, SEC2 was able to redirect the differentiation of BMSCs from adipogenesis to osteogenesis, thus counteracting the bone loss and bone marrow adiposity induced by SMG. Our research also demonstrated that

SEC2 achieves this rescuing effect by activating the ERK/ $\beta$ -catenin signaling pathways, as evidenced by increased Erk phosphorylation and  $\beta$ -catenin nucleus translocation. Importantly, when  $\beta$ -catenin was silenced using siRNA, the regulatory effect of SEC2 was diminished. These findings reveal a novel mechanism by which SEC2 regulates the fate of BMSCs between adipogenesis and osteogenesis under microgravity conditions, highlighting its potential as a therapeutic approach for the management of bone loss and bone marrow adiposity in microgravity environments.

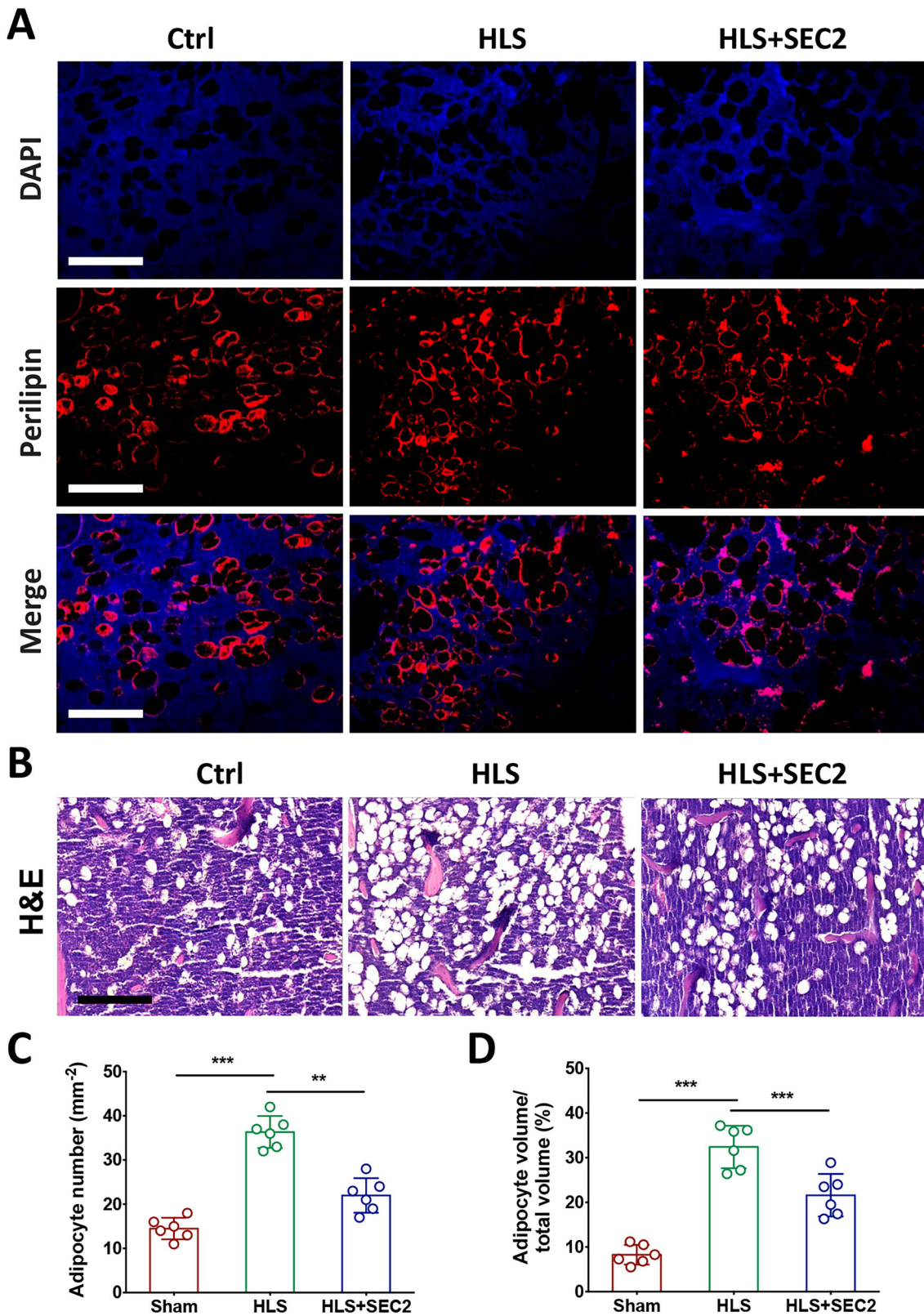
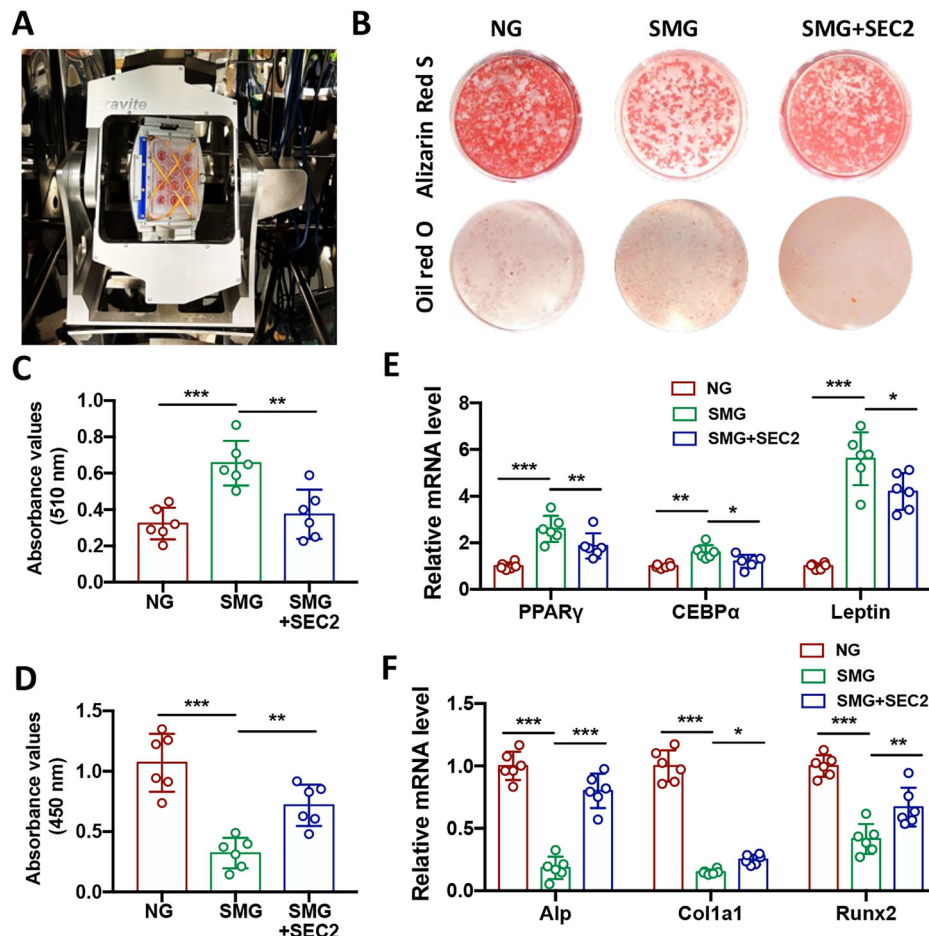


**Fig. 2 | SEC2 reversed microgravity enhanced bone marrow adiposity.** A Femurs isolated from Control, HLS and HLS+SEC2 were subjected IF staining using anti-perilipin antibody. Representative images of perilipin-stained femurs isolated from three groups of mice. Scale bar: 100  $\mu\text{M}$ . B Femur subjected to hematoxylin & eosin

staining. Representative images of hematoxylin & eosin-stained femurs harvested from Control, HLS and HLS+SEC2 groups. Scale bar: 100  $\mu\text{M}$ . C, D Quantification of bone marrow adipocyte number and percentage of adipocyte volume based on hematoxylin & eosin staining ( $n = 6$ ;  $^*p < 0.05$ ,  $^{**}p < 0.01$ ,  $^{***}p < 0.001$ ).

**Fig. 3 | SEC2 reversed microgravity induced BMSCs trans-differentiation from osteogenesis to adipogenesis.** A Three-dimensional random positioning machine (RPM) for inducing simulated microgravity on BMSCs. RPM setup was used to continuously make random changes in the orientation of BMSCs relative to the gravity vector. B Representative images of Oil red O or Alizarin red S staining of BMSCs cultured in 1:1 OB/AD induction medium under mimicked microgravity and treated with SEC2. C Quantification of lipid accumulation by measuring the 518 nm absorbance after eluting the Oil Red O deposit with isopropanol. D Quantification of Alizarin Red S stained nodulus measured under the wavelength of 560 nm. The mRNA expression level of adipogenesis markers (E) and osteogenesis markers (F) were measured by real-time PCR.



Microgravity is a crucial factor that affects various physiological systems of the human body when exposed to the space environment. These effects become more pronounced over time. A specific symptom induced by long-term spaceflight is bone loss, which is partially attributed to changes in the behavior of bone cells<sup>7</sup>. Bone cells play a significant role in bone remodeling, with osteoblasts responsible for bone formation, osteoclasts for bone resorption, and osteocytes acting as regulators of bone remodeling and mineral balance<sup>8</sup>. The experienced weightlessness in microgravity decreases the stress on load-bearing bones, leading to adaptive modifications that promote bone resorption and hinder new bone formation<sup>9</sup>. Prior research has emphasized the importance of exposure to different biochemical and biomechanical factors in determining the fate of BMSCs. Prolonged bed rest, resulting from brain/spinal cord injury or space travel, can lead to a lack of mechanical signals. This absence redirects the differentiation of BMSCs from osteogenesis to adipogenesis, ultimately leading to disuse osteoporosis<sup>10</sup>. Observations among patients with osteoporosis have shown that there is a tendency for BMSCs to differentiate into adipocytes rather than osteoblasts. This results in the accumulation of adipose tissue within the bone marrow and irregular bone reconstruction<sup>11</sup>. The in vitro study result showed that the microgravity condition inhibits the BMSCs osteogenesis and instead induces the development of adipocytes<sup>12</sup>. However, mechanical loading has the opposite effect by promoting osteogenesis over adipogenesis, which is achieved by downregulating the expression of PPAR $\gamma$ <sup>13</sup>. Furthermore, with the facilities availability, Wang's group investigated the effects of real microgravity using a scientific satellite and discovered that microgravity in space leads to the trans-differentiation of BMSCs from osteogenesis to adipogenesis. This is achieved by suppressing the BMP2/SMAD and integrin/FAK/ERK signaling pathways, which in turn decreases the expression and activity of RUNX2, a transcription factor

involved in osteogenesis. Additionally, microgravity increases the p38/MAPK signaling pathway and decreases the ERK/AKT signaling pathway, thus promoting adipogenesis<sup>4</sup>. In our study, we used a rotating random position system to simulate the microgravity environment. The constant rotation of the sample may result in the time averaging of the g vector to near 0<sup>14</sup>. However, it is important to note that our system does not entirely eliminate gravity, representing a limitation of our study. Additionally, the movement of the cell culture medium within the culture reservoir, driven by the rotation of our SMG system, may produce fluid shear forces on the cells. These forces could potentially trigger unintended signaling pathways and induce cell behaviors that might not occur in true microgravity conditions. Nevertheless, our SMG study results have shown a decrease in osteogenesis and an increase in adipogenesis of BMSCs. These findings are consistent with previous studies and confirm the reliability of our system in interpreting the effect of microgravity on in vitro tissue culture.

*Staphylococcus aureus* is a Gram-positive bacterium that produces a heat-resistant enterotoxin called SEC2. SEC2 is categorized as a superantigen and has the ability to activate T cells by interacting with major histocompatibility class II (MHC II) molecules, leading to downstream immune reactivity. The stimulation of immune cells by SEC2 results in the release of inflammatory cytokines, including IFN $\gamma$ , IL-1, IL-6, and TNF $\alpha$ , which exhibit various anti-cancer properties<sup>15,16</sup>. Additionally, the increased levels of IFN $\gamma$  triggered by SEC2 enhance the production of nitric oxide and activate the p38/MAPK signaling pathway, ultimately promoting the osteogenesis of BMSCs by upregulating the expression of Runx2<sup>17</sup>. Moreover, SEC2 has been found to directly promote BMSCs osteogenesis and accelerate bone fracture healing<sup>18</sup>, as well as promote bone consolidation in the distraction osteogenesis model<sup>19</sup>. Fu's team made the discovery that SEC2 activates BMP2 and Runx2 signaling pathways to promote

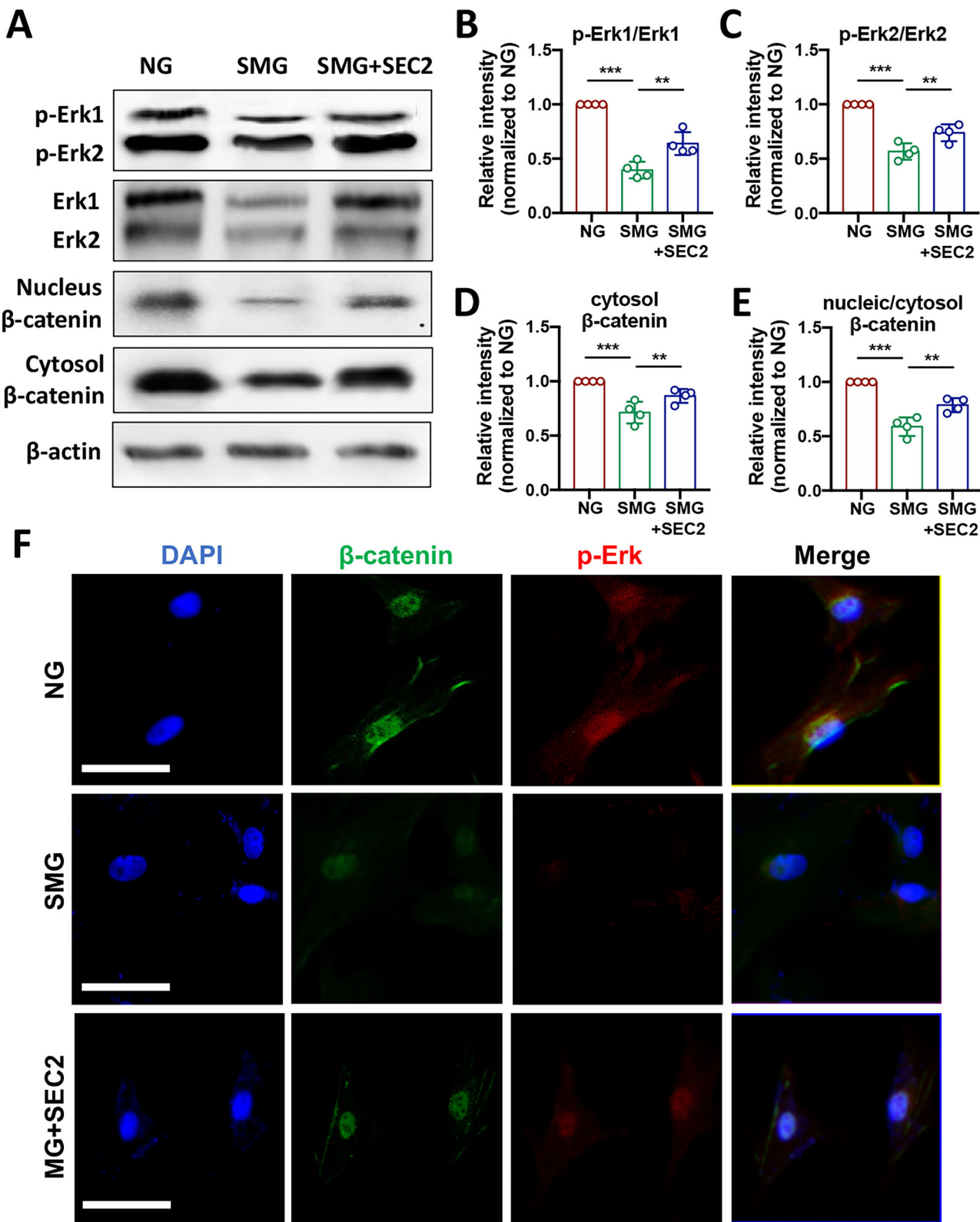
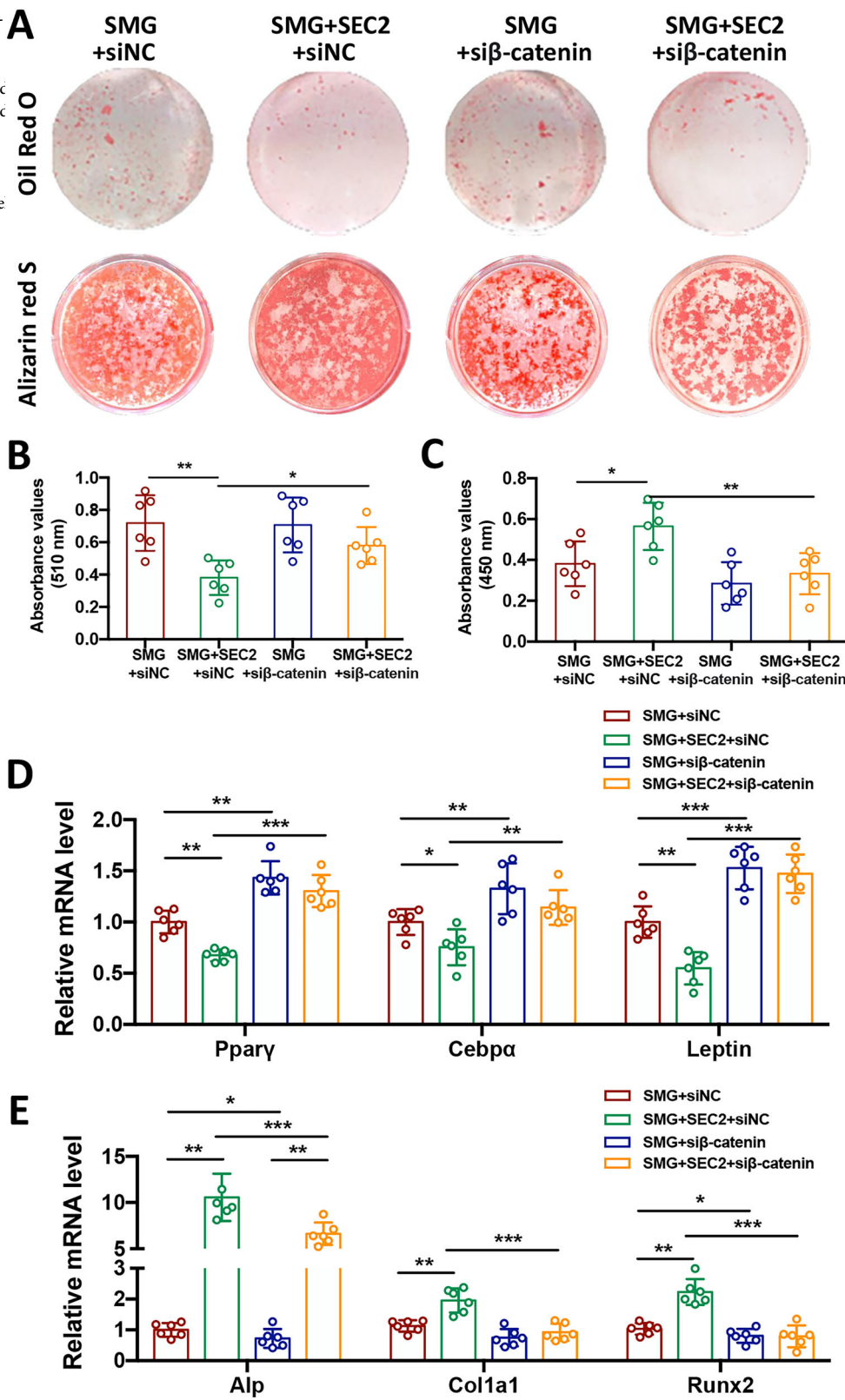


**Fig. 4 | SEC2 reversed microgravity induced down-regulation of ERK and β-catenin signaling.** A Western blot analysis of Erk phosphorylation and β-catenin nucleus translocation of BMSCs under SMG condition and SEC2 treatment. Quantitative analysis of relative protein band intensity of p-Erk1/Erk1 (B), p-Erk2/

Erk2 (C), cytosol β-catenin (D) and nucleic/cytosol β-catenin (E). F Immunofluorescence (IF) staining analysis of β-catenin and Erk nucleus translocation under SMG condition and treated with SEC2. Scale bar: 50  $\mu$ m.

**Fig. 5 | SEC2 reversed microgravity induced adipogenesis and impaired osteogenesis of BMSCs via downregulating  $\beta$ -catenin expression.**

A Representative images of Oil red O or Alizarin red S staining of BMSCs after  $\beta$ -catenin knockdown and cultured in 1:1 OB/AD induction medium under mimicked microgravity and treated with SEC2. Quantitative analysis of Oil Red O (B) and ARS staining intensities (C). The mRNA expression levels of adipogenesis (D) and osteogenesis markers (E) measured by real-time PCR ( $n = 6$ ; \* $p < 0.05$ , \*\* $p < 0.01$ , \*\*\* $p < 0.001$ ).



osteogenesis. Additionally, SEC2 administration induces the expression of IFI6, a gene that is induced by IFN $\gamma$ , which further enhances the commitment of BMSCs to osteogenesis<sup>20</sup>. Our research primarily focused on elucidating the mechanism of SEC2 in microgravity-induced osteoporosis, given its potential to markedly influence bone regeneration. In contrast, osteocytes, which are the most abundant bone cells, serve as central

regulators of bone homeostasis by sensing mechanical stress and modulating osteoblast and osteoclast activity through molecules like sclerostin and RANKL. Under microgravity conditions, reduced mechanical loading leads osteocytes to increase RANKL secretion, promoting osteoclastogenesis and bone resorption, which exacerbates bone loss. The cytokine storm induced by SEC2, particularly IL-6 and TNF $\alpha$ , could further dysregulate

osteocyte signaling by elevating RANKL expression, thereby amplifying osteoclast activity and bone degradation in microgravity environments. Therefore, it is crucial to thoroughly understand the role of SEC2 in bone homeostasis to develop targeted therapies, and if any exist, to identify potential adverse effects of such therapies in counteracting microgravity-induced bone loss.

In our study, we discovered that the SMG condition deactivated Erk phosphorylation as well as  $\beta$ -catenin expression and nucleus translocation in BMSCs. The administration of SEC2 partially counteracted the negative effects of SMG on the Erk/ $\beta$ -catenin signaling. Knockdown of  $\beta$ -catenin could significantly hinder the enhancing effect of SEC2 on BMSCs' osteogenic differentiation under SMG. Both the ERK and Wnt/ $\beta$ -catenin signaling pathways played crucial roles in managing BMSCs differentiation. Specifically, the ERK/MAPK pathways contributed to osteoblast differentiation by phosphorylating and activating RUNX2, a major transcription factor that regulates downstream signaling pathways during osteoblastic differentiation<sup>21</sup>. On the contrary, it is evident that Wnt/ $\beta$ -catenin signaling is crucial in determining the lineage of mesenchymal precursor cells during their growth phase.  $\beta$ -catenin, a key component of canonical Wnt signaling, has a significant influence in determining the cell fate of BMSCs. Research demonstrated that the elimination of  $\beta$ -catenin in pre-osteoblasts led to a shift in cell fate from osteoblasts to adipocytes, as observed through lineage tracing. This shift may potentially result in an increase in bone marrow adiposity and a decrease in bone mass<sup>22</sup>. A study on irisin, a small molecule, revealed that it could rescue the impaired osteoblast differentiation under SMG by increasing  $\beta$ -catenin expression. This finding further confirms the significant role of Wnt/ $\beta$ -catenin signaling in regulating osteogenesis under microgravity<sup>23</sup>. Furthermore, the crosstalk between the Wnt/ $\beta$ -catenin and ERK signaling pathways in microgravity conditions was also examined. Cheng et al. discovered that SMG inhibits both Wnt/ $\beta$ -catenin and ERK signaling. Interestingly, the introduction of the ERK agonist tert-Butylhydroquinone (tBHQ) was able to activate Wnt/ $\beta$ -catenin to a similar extent as the Wnt activator LiCl, which suggests the presence of a regulatory cascade involving ERK-Wnt/ $\beta$ -catenin in response to SMG stimulation<sup>6</sup>. In our own study, we confirmed that both ERK and Wnt/ $\beta$ -catenin signaling in BMSCs were suppressed under SMG conditions but were enhanced with SEC2 treatment. However, we haven't fully characterized the potential cell surface receptor for SEC2 on BMSCs. Emerging evidence suggested that SEC2 may interact with Toll-like receptors (TLRs), particularly TLR2 and TLR4, on the surface of various cell types, including BMSCs. These receptors can initiate downstream signaling cascades that activate ERK and  $\beta$ -catenin pathways<sup>24</sup>. Further investigations are needed to fully understand the engagement of TLRs in regulatory mechanism of SEC2 on the ERK and Wnt/ $\beta$ -catenin signaling pathways during BMSCs osteogenesis and adipogenesis under SMG. This suggests that SEC2 may exert its osteogenic effects through binding to TLRs or similar pattern recognition receptors on BMSCs, triggering ERK and  $\beta$ -catenin signaling pathways that facilitate osteogenic differentiation and bone regeneration.

During the early phase of space exploration, NASA discovered that bisphosphonates, commonly used for osteoporosis treatment, effectively slowed the progression of osteoporosis in astronauts, enabling them to spend more time in space. However, these medications do come with side effects<sup>25</sup>. In 2001, a partnership between Amgen and NASA led to the testing of a sclerostin antibody drug called STS-108 on animals aboard a spacecraft. The results were promising, showing a reduction in bone loss in microgravity conditions<sup>26</sup>. More recently, researchers at UCLA reported that a drug named BP-NELL-PEG successfully inhibited spaceflight-induced bone loss in mice aboard the International Space Station, notably without any adverse effects<sup>27</sup>. At the same time, during the launch of China's "Tianzhou-1" spacecraft, Tsinghua University introduced an anti-osteoporosis drug known as 3-hydroxybutyrate (3HB), which has the potential to enhance the proliferation, differentiation, and mineralization of osteoblasts while inhibiting the abnormal activation of osteoclasts<sup>28</sup>. SEC2 is a specifically designed fracture healing medication characterized by a low effective dose and cost-effectiveness, boasting a stable molecular

composition that allows for storage at ambient temperatures. Unlike protein-based and nucleic acid medications, SEC2 offers significant advantages in storage and transportation, making it particularly well-suited for the needs of space exploration.

However, our study still has a limitation. While we discussed the effects of SEC2 on T cells, it does not sufficiently address how microgravity conditions might influence this interaction or result in indirect effects. Microgravity is known to significantly alter immune cell functions, including T cell activation, proliferation, and cytokine production<sup>29</sup>. Notably, Risso's research demonstrated a substantial reduction in the secretion of IL-2 and IFN $\gamma$  by human and animal T cells under microgravity conditions<sup>30</sup>. Although our previous work indicated that SEC2 stimulates T cells to produce IFN $\gamma$ , a cytokine essential for bone formation<sup>17</sup>, further research is necessary to explore how SEC2 may indirectly promote bone regeneration through T cell-mediated mechanisms in a microgravity environment. Such studies could strength our understanding of the complex immunological landscape and elucidate the comprehensive effects of SEC2 under microgravity conditions.

Overall, in our study, we successfully demonstrated the potential of SEC2 administration in rescuing bone loss and bone marrow adiposity caused by hind limb suspension, a simulation of microgravity. Additionally, we investigated the mechanism of SEC2 in inhibiting the transdifferentiation of BMSCs from osteogenesis to adipogenesis under SMG. Notably, we found that the ERK/ $\beta$ -catenin signaling pathway played a critical role in the regulatory effect of SEC2 on BMSCs' cell fate commitment under SMG conditions. These findings suggest that SEC2 could be a promising treatment approach and offer a novel therapy for preventing osteoporosis and other musculoskeletal disorders induced by microgravity.

## Methods

### Hind limb unloading

The methodology for the hindlimb unloading model was adapted from Morey-Holton's original protocol. In general, a total of 18 6-week-old C57BL/6 male mice were divided into three groups: the control group, HLS group, and HLS+SEC2 group. The mice in the control group were allowed to move freely without hindlimb unloading. The mice in the HLS or HLS+SEC2 groups were housed in cages and suspended to unload their hindlimbs, following the recommendations of Morey-Holton. This positioning held their bodies at an approximate angle of 30°<sup>31</sup>. This setup provided the mice with unlimited access to food and water, ensuring their nutritional and hydration needs were met. The mice's appearance, eating and drinking patterns, and tail conditions were monitored twice daily. In the HLS+SEC2 groups, the SEC2 was injected into the HLS mice intraperitoneally at a dosage of 10  $\mu$ g/kg twice a week. After a 2-week suspension period, the mice were euthanized, and their bilateral femurs were collected for further analysis. All experimental procedures conducted in this study were approved by the Ethics Committee of the Chinese University of Hong Kong and followed the guidelines set by the Hong Kong Animal Experimentation Ethics Committee (AEEC).

### Micro-CT analysis

The femurs were placed in a 15-mm imaging cylinder and fully submerged in 70% ethanol. They were then analyzed using micro-CT (Scanco Medical, Wangen, Switzerland) with the following parameters: voltage at 70 kV, isotropic resolution at 10.5  $\mu$ m, and reconstruction threshold at 158 mg hydroxyapatite/cm<sup>3</sup>. The volume of interest within the distal femurs was determined, starting from the growth plate and extending for 200 successive sections (10  $\mu$ m/section) on the proximal side. Three-dimensional (3D) reconstructions were generated, and bone parameters such as bone volume to total volume (BV/TV), bone marrow density (BMD), and trabecular thickness (Tb.Th.) were calculated using established methods<sup>32</sup>.

### H&E and immunohistochemistry

Hindlimb femurs from different mice groups were collected and equilibrated with 4% paraformaldehyde overnight. Subsequently, the femurs were

decalcified with 5% ethylenediaminetetraacetic acid (EDTA) at room temperature for 3 weeks. After dehydration and paraffin embedding, the femurs were longitudinally sectioned at a thickness of 4  $\mu\text{m}$ . The sections were then subjected to hematoxylin & eosin (H&E) staining for the semi-quantitative analysis of proximal metaphyseal adipocyte parameters, including adipocyte number ( $\text{mm}^{-2}$ ) and adipocyte volume per tissue volume (AV/TV). The immunohistochemistry (IHC) staining was performed according to an established protocol<sup>33</sup>. For IHC staining, primary antibodies including rabbit anti-OCN (1:100, ab93876, Abcam, Cambridge, UK) and rabbit anti-OPN (1:100, ab8468, Abcam, Cambridge, UK) were utilized in accordance with the manufacturer's instructions. Signal detection was achieved using the horseradish peroxidase-streptavidin system (Dako, Carpinteria, USA), with hematoxylin used for counterstaining. Positive staining images of the trabecular bones at the distal metaphysis were captured using a light microscope (Leica, Cambridge, UK).

### Rotation microgravity simulation

Gravite® desktop random positioning machine (RPM, Space Bio-Laboratories Co., Ltd, Hiroshima, Japan) was used to simulate microgravity conditions for cell culture following previous reports<sup>34</sup>. To investigate the effects of SMG, BMSCs were cultured in a 12-well culture dish until 90% confluence. The dish was then covered with a 12-well i-TEC® Well Plate Cover (Sanplatec, Osaka, Japan) and securely fixed onto the cell culture container of the RPM using rubber bands. The cell culture container, along with the RPM's internal framework, was placed within a 37 °C incubator. The machine was operated in a random mode, with speeds ranging from 8 to 12 rpm and directions that encompassed both the inner and outer frames. This created a simulated environment of  $10^{-3}\text{g}$ , as confirmed by a gravity acceleration sensor. A stationary gravity control group was set with the BMSCs cultured in the same RPM positioned incubator without rotation.

### BMSCs culture and differentiation

BMSCs were isolated from the bone marrow of 6-week-old C57BL/6 mice and stored in our lab, following the previously described method<sup>35</sup>. The culture medium consisted of Minimum Essential Medium alpha (α-MEM) supplemented with 10% fetal bovine serum and a mixture of 1% penicillin, streptomycin and neomycin. The cells were cultured in a humidified environment at 37 °C with 5% CO<sub>2</sub>. For our study, a combination of osteoblastogenesis (OB) and adipogenesis (AD) induction medium was used at a 1:1 ratio. The OB induction medium contained the culture medium supplemented with 10 nM dexamethasone, 50  $\mu\text{g}/\text{mL}$  ascorbic acid, and 10 mM glycerol 2-phosphate. The AD induction medium was prepared by adding 500 nM dexamethasone, 50  $\mu\text{M}$  indomethacin, 0.5 mM isobutyl methylxanthine, and 10  $\mu\text{g}/\text{mL}$  insulin to the culture medium. The induction of BMSCs was performed for 7 days using the OB:AD induction medium. The combined induction medium was replaced every 3 days. In the SEC2 treatment group, SEC2 was added to the BMSCs' induction medium at a concentration of 10  $\mu\text{g}/\text{mL}$ , following the previously described method<sup>20</sup>.

### Immunofluorescence (IF) staining

For immunofluorescence (IF) staining, BMSCs were cultured in a 12-well plate until 80% confluence. The cells were then treated with SEC2 (10  $\mu\text{g}/\text{mL}$ ) and fixed on the RPM SMG system for 12 h. After incubation, the cells were PBS washed and fixed with a 4% phosphate paraformaldehyde solution (Sigma-Aldrich, St. Louis, MO, USA). To block nonspecific binding, the cells were blocked with 5% BSA. For paraffin sections, the sections were boiled in 100 °C citrate buffer for antigen retrieval, and then soaked in hydrogen peroxide for quenching. After that, the sections were blocked with 3% BSA. The fixed cells or sections were incubated overnight at 4 °C with primary antibodies, including rabbit anti-perilipin (1:200, ab3526, Abcam, Cambridge, UK), mouse anti- $\beta$ -catenin (1:100, 610153, BD Biosciences, San Jose, CA, USA) and rabbit anti-Erk (1:100, Sc-16982, Santa Cruz Biotechnology, Santa Cruz, CA, USA), in BSA. Subsequently, cells were

incubated with secondary antibodies including goat anti-rabbit IgG-H&L (Alexa Fluor® 488) (ab150077, Abcam, Cambridge, UK) and goat anti-rabbit IgG-H&L (Alexa Fluor® 647) (ab150083, Abcam, Cambridge, UK) according to the primary antibody used. The cells or sections were counterstained with DAPI. Photographs of selected areas were taken under a Leica DMIRB Inverted Leica Modulation Contrast Microscope (Leica, Wetzlar, Germany).

### Oil Red O and Alizarin Red S staining

To perform Oil Red O staining, the cells in the culture plate were washed with PBS and fixed with 4% paraformaldehyde for 30 min. After PBS washing, 200  $\mu\text{l}$  of a 0.5% Oil Red O solution (ORO, Sigma-Aldrich, St. Louis, MO, USA) was added to the fixed cells and incubated at room temperature for 30 min. The ORO staining patterns were then fixed with 70% ethanol and washed with PBS. For Alizarin Red S staining, the mouse cells were washed with PBS and fixed with 70% ethanol for 30 min. The cells were then stained with a 2% Alizarin Red S staining solution (ARS, Merck, Rahway, NJ, USA) for 10 min. The stained lipid droplets or calcified nodules were captured using an Epson Perfection V850 scanner (Seiko Epson, Japan) and the quantitative analysis was performed using ImageJ (NIH, Bethesda, MD, USA)<sup>36</sup>.

### Real-time PCR

Total RNA of cultured cells was collected using the RNAiso Plus reagent (TaKaRa, Shiga, Japan) following the manufacturer's instructions. Following RNA extraction, cDNAs were reversely synthesized from the RNA samples using PrimeScript RT Master Mix (TaKaRa, Shiga, Japan). For quantifying the expression of target mRNA, real-time PCR was performed using Power SYBR Green PCR Master Mix (Thermo Fisher Scientific, Mass, IL, USA) with the ABI 7300 Fast Real-Time PCR Systems (Applied Biosystems, Foster, CA, USA). The relative fold changes of the candidate gene expression were subsequently determined by employing the  $2^{-\Delta\Delta\text{Ct}}$  method. The primers used in the study were listed in Supplementary Table 1.

### Western blot

Cells were lysed using the radioimmunoprecipitation assay (RIPA) buffer, which consists of 25 mM Tris-Cl (pH 8.0), 150 mM NaCl, 0.1% SDS, 0.5% sodium deoxycholate, 1% NP40, and cOmplete Mini Protease Inhibitor Cocktail (Roche, Basel, Swiss) was added. The lysed cells were then centrifuged at 14,000 rpm for 10 min at 4 °C to obtain the soluble protein fraction. The soluble proteins were mixed with 5× sample loading buffer (Roche, Basel, Swiss). The protein samples were loaded onto sodium dodecyl sulfate-polyacrylamide gel electrophoresis (SDS-PAGE) gel and subjected to electrophoresis at 120 V, and then transferred onto a polyvinylidene fluoride membrane at 100 V for 1 h at 4 °C. Membranes were first blocked with 5% nonfat milk. Then, specific antibodies were applied and incubated: mouse anti- $\beta$ -catenin (1:3000, 610153, BD Biosciences, San Jose, CA, USA), rabbit anti-Erk (1:1000, Sc-16982, Santa Cruz Biotechnology, Santa Cruz, CA, USA), mouse anti-phosphorylated Erk (610030, BD Biosciences, San Jose, CA, USA), and rabbit anti- $\beta$ -actin (1:3000, Sc-47778, Santa Cruz Biotechnology, Santa Cruz, CA, USA). The results were captured on an X-ray film using a Kodak film developer (Fujifilm, Tokyo, Japan). The integrated gray values for each band were then quantified using ImageJ software (NIH, Bethesda, MD, USA).

### Statistical analysis

All data were presented as mean  $\pm$  standard deviations. The experiments were independently repeated at least three times, and representative data are shown. The statistical significance among multiple groups was assessed using One-way ANOVA for comparisons, followed by Tukey's Honestly Significant Difference test for post-hoc analysis. The statistical significance between two independent groups was evaluated using Two-tailed student's *t*-test with Welch's correction. The analysis was performed with GraphPad

Prism 8 (GraphPad Software, USA). A *p*-value of less than 0.05 was considered statistically significant.

## Data availability

Raw data were generated at the Chinese University of Hong Kong. Derived data supporting the findings of this study are available from the corresponding author GL on request.

Received: 7 March 2025; Accepted: 21 November 2025;

Published online: 07 December 2025

## References

- Wronski, T. J., Morey-Holton, E. & Jee, W. S. Skeletal alterations in rats during space flight. *Adv. Space Res.* **1**, 135–140 (1981).
- LeBlanc, A., Rowe, R., Schneider, V., Evans, H. & Hedrick, T. Regional muscle loss after short duration spaceflight. *Aviat. Space Environ. Med.* **66**, 1151–1154 (1995).
- Baio, J. et al. Cardiovascular progenitor cells cultured aboard the International Space Station exhibit altered developmental and functional properties. *NPJ Microgravity* **4**, 13 (2018).
- Zhang, C. et al. Space microgravity drives transdifferentiation of human bone marrow-derived mesenchymal stem cells from osteogenesis to adipogenesis. *FASEB J.* **32**, 4444–4458 (2018).
- Wang, H. et al. Low-dose staphylococcal enterotoxin C2 mutant maintains bone homeostasis via regulating crosstalk between bone formation and host T-cell effector immunity. *Adv. Sci.* **10**, e2300989 (2023)..
- Cheng, Y., Zhou, Y., Lv, W., Luo, Q. & Song, G. Simulated microgravity inhibits rodent dermal fibroblastic differentiation of mesenchymal stem cells by suppressing ERK/beta-catenin signaling pathway. *Int. J. Mol. Sci.* **22**, 10702 (2021).
- Vico, L. & Hargens, A. Skeletal changes during and after spaceflight. *Nat. Rev. Rheumatol.* **14**, 229–245 (2018).
- Wang, L., You, X., Zhang, L., Zhang, C. & Zou, W. Mechanical regulation of bone remodeling. *Bone Res.* **10**, 16 (2022).
- Man, J., Graham, T., Squires-Donelly, G. & Laslett, A. L. The effects of microgravity on bone structure and function. *NPJ Microgravity* **8**, 9 (2022).
- Yamazaki, S. et al. Regulation of osteogenetic differentiation of mesenchymal stem cells by two axial rotational culture. *J. Artif. Organs* **14**, 310–317 (2011).
- Chen, Q. et al. Fate decision of mesenchymal stem cells: adipocytes or osteoblasts?. *Cell Death Differ.* **23**, 1128–1139 (2016).
- Zayzafoon, M., Gathings, W. E. & McDonald, J. M. Modeled microgravity inhibits osteogenic differentiation of human mesenchymal stem cells and increases adipogenesis. *Endocrinology* **145**, 2421–2432 (2004).
- David, V. et al. Mechanical loading down-regulates peroxisome proliferator-activated receptor gamma in bone marrow stromal cells and favors osteoblastogenesis at the expense of adipogenesis. *Endocrinology* **148**, 2553–2562 (2007).
- Klaus, D. M. Clinostats and bioreactors. *Gravit. Space Biol. Bull.* **14**, 55–64 (2001).
- Liu, T. et al. Superantigen staphylococcal enterotoxin C1 inhibits the growth of bladder cancer. *Biosci. Biotechnol. Biochem.* **81**, 1741–1746 (2017).
- Liu, Y. et al. SEC2-induced superantigen and antitumor activity is regulated through calcineurin. *Appl. Microbiol Biotechnol.* **97**, 9695–9703 (2013).
- Wang, H. et al. Low-dose Staphylococcal Enterotoxin C2 mutant maintains bone homeostasis via regulating crosstalk between bone formation and host T-cell effector immunity. *Adv. Sci.* **10**, e2300989 (2023).
- Wu, T. et al. Staphylococcal enterotoxin C2 promotes osteogenesis of mesenchymal stem cells and accelerates fracture healing. *Bone Jt. Res.* **7**, 179–186 (2018).
- Xu, J. et al. Staphylococcal enterotoxin C2 expedites bone consolidation in distraction osteogenesis. *J. Orthop. Res.* **35**, 1215–1225 (2017).
- Fu, W. M. et al. Staphylococcal enterotoxin C2 promotes osteogenesis and suppresses osteoclastogenesis of human mesenchymal stem cells. *Exp. Cell Res.* **322**, 202–207 (2014).
- Franceschi, R. T. & Xiao, G. Regulation of the osteoblast-specific transcription factor, Runx2: responsiveness to multiple signal transduction pathways. *J. Cell Biochem.* **88**, 446–454 (2003).
- Song, L. et al. Loss of Wnt/beta-catenin signaling causes cell fate shift of preosteoblasts from osteoblasts to adipocytes. *J. Bone Min. Res.* **27**, 2344–2358 (2012).
- Chen, Z. et al. Recombinant Irisin prevents the reduction of osteoblast differentiation induced by stimulated microgravity through increasing beta-catenin expression. *Int. J. Mol. Sci.* **21**, 1259 (2020).
- Kassem, A., Lindholm, C. & Lerner, U. H. Toll-like receptor 2 stimulation of osteoblasts mediates *Staphylococcus aureus* induced bone resorption and osteoclastogenesis through enhanced RANKL. *PLoS ONE* **11**, e0156708 (2016).
- Rosenthal, R., Schneider, V. S., Jones, J. A. & Sibonga, J. D. The case for bisphosphonate use in astronauts flying long-duration missions. *Cells* **13** <https://doi.org/10.3390/cells13161337> (2024).
- Yu, S. et al. Drug discovery of sclerostin inhibitors. *Acta Pharm. Sin. B* **12**, 2150–2170 (2022).
- Ha, P. et al. Bisphosphonate conjugation enhances the bone-specificity of NELL-1-based systemic therapy for spaceflight-induced bone loss in mice. *NPJ Microgravity* **9**, 75 (2023).
- Cao, Q. et al. The mechanism of anti-osteoporosis effects of 3-hydroxybutyrate and derivatives under simulated microgravity. *Biomaterials* **35**, 8273–8283 (2014).
- Spatz, J. M. et al. Human immune system adaptations to simulated microgravity revealed by single-cell mass cytometry. *Sci. Rep.* **11**, 11872 (2021).
- Risso, A. et al. Activation of human T lymphocytes under conditions similar to those that occur during exposure to microgravity: a proteomics study. *Proteomics* **5**, 1827–1837 (2005).
- Morey-Holton, E. R. & Globus, R. K. Hindlimb unloading rodent model: technical aspects. *J. Appl Physiol.* **92**, 1367–1377 (2002).
- Shi, L. et al. Vasoactive intestinal peptide promotes fracture healing in sympathectomized mice. *Calcif. Tissue Int.* **109**, 55–65 (2021).
- Sun, Y. et al. mir-21 overexpressing mesenchymal stem cells accelerate fracture healing in a rat closed femur fracture model. *Biomed. Res. Int.* **2015**, 412327 (2015).
- Imura, T., Nakagawa, K., Kawahara, Y. & Yuge, L. Stem cell culture in microgravity and its application in cell-based therapy. *Stem Cells Dev.* **27**, 1298–1302 (2018).
- Feng, L. et al. MicroRNA-378 suppressed osteogenesis of MSCs and impaired bone formation via inactivating Wnt/beta-catenin signaling. *Mol. Ther. Nucleic Acids* **21**, 1017–1028 (2020).
- Zhang, J. F. et al. MiRNA-20a promotes osteogenic differentiation of human mesenchymal stem cells by co-regulating BMP signaling. *RNA Biol.* **8**, 829–838 (2011).

## Acknowledgements

This work was supported by grants from the National Natural Science Foundation of China (82172430 and 82272505), University Grants Committee, Research Grants Council of the Hong Kong Special Administrative Region, China (14108720, 14121721, 14202920, N\_CUHK472/22, C7030-18G, T13-402/17-N and AoE/M-402/20), Health Medical Research Fund (HMRF) Hong Kong (17180831, 08190416 and 09203436), Hong Kong Innovation Technology Commission Funds (PRP/

050/19FX). This study also received support from the research funds from Health@InnoHK program launched by Innovation Technology Commission of the Hong Kong SAR, PR China.

### Author contributions

N.H., L.F., and G.L. designed the study; N.H., Z.Y., H.W., X.L., S.B., and Y.W. performed the experiments and acquired the data; N.H., Z.Y., and S.L. analyzed and interpreted the data; N.H. drafted the manuscript; L.F. performed the revision; G.L. and M.D. finalized and approved the manuscript for submission.

### Competing interests

The authors declare no competing interests.

### Additional information

**Supplementary information** The online version contains supplementary material available at <https://doi.org/10.1038/s41526-025-00548-y>.

**Correspondence** and requests for materials should be addressed to Micky D. Tortorella, Lu Feng or Gang Li.

**Reprints and permissions information** is available at <http://www.nature.com/reprints>

**Publisher's note** Springer Nature remains neutral with regard to jurisdictional claims in published maps and institutional affiliations.

**Open Access** This article is licensed under a Creative Commons Attribution-NonCommercial-NoDerivatives 4.0 International License, which permits any non-commercial use, sharing, distribution and reproduction in any medium or format, as long as you give appropriate credit to the original author(s) and the source, provide a link to the Creative Commons licence, and indicate if you modified the licensed material. You do not have permission under this licence to share adapted material derived from this article or parts of it. The images or other third party material in this article are included in the article's Creative Commons licence, unless indicated otherwise in a credit line to the material. If material is not included in the article's Creative Commons licence and your intended use is not permitted by statutory regulation or exceeds the permitted use, you will need to obtain permission directly from the copyright holder. To view a copy of this licence, visit <http://creativecommons.org/licenses/by-nc-nd/4.0/>.

© The Author(s) 2025